

See discussions, stats, and author profiles for this publication at: <https://www.researchgate.net/publication/237146472>

Weak Ion–Molecule Interactions in the Gas Phase: A High–Pressure Mass Spectrometry and Computational Study of Chloride–Alkane Interactions

ARTICLE in THE JOURNAL OF PHYSICAL CHEMISTRY A · JUNE 2013

Impact Factor: 2.69 · DOI: 10.1021/jp403422q · Source: PubMed

READS

57

4 AUTHORS, INCLUDING:



Blake E Ziegler

University of Waterloo

9 PUBLICATIONS 33 CITATIONS

SEE PROFILE



Tanya Gamble

AB SCIEX

8 PUBLICATIONS 91 CITATIONS

SEE PROFILE



Terrance McMahon

University of Waterloo

206 PUBLICATIONS 5,451 CITATIONS

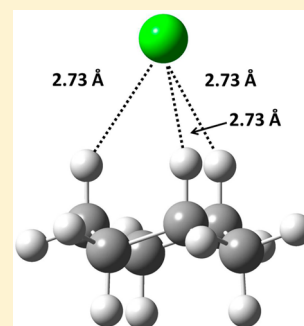
SEE PROFILE

Weak Ion–Molecule Interactions in the Gas Phase: A High-Pressure Mass Spectrometry and Computational Study of Chloride–Alkane Interactions

Blake E. Ziegler, Tanya N. Gamble, Chun Li, and Terry B. McMahon*

Department of Chemistry, University of Waterloo, Waterloo, Ontario, Canada N2L 3G1

ABSTRACT: High-pressure mass spectrometric equilibrium experiments and electronic structure calculations have been carried out to investigate the energetics of the interactions of chloride ion with a series of normal alkanes and cycloalkanes in the gas phase. The structures of the complexes obtained from the electronic structure calculations provide considerable insight into the nature of the interaction between the negatively charged ion and the alkanes, which has the character of a purely ion-induced dipole interaction. The structural information also shows how the charged species affect the conformation of the normal alkanes.



■ INTRODUCTION

The solubility of ionic species is driven by the extent to which the separated ionic species of an ionic salt interact with the solvent medium. For example, sodium chloride dissolves very readily in water because the magnitude of the interaction between sodium ions and water molecules and chloride ions and water molecules can readily overcome the lattice energy of the ionic solid. In the case of sodium ion, the sodium cation is able to interact very strongly with the dipole moment of a single water molecule, while, similarly, the chloride ion interacts very favorably with a local O–H bond dipole to effectively form a hydrogen bond. Subsequent addition of further molecules of water to the singly solvated ions results in the fully hydrated species. Thus, sodium chloride is exceedingly soluble in water. As the dipole moment of solvent molecules is diminished, and/or the hydrogen bonding possibilities are reduced, weaker solvation interactions result, leading to lower solubility of ionic species. For example, solvents such as acetonitrile and dimethyl sulfoxide (DMSO) are classified as dipolar aprotic solvents, and these solvents are frequently used to reveal intrinsic stabilities of ions by minimizing solvation effects, particularly those due to hydrogen bonding. In the extreme, nonpolar aprotic solvents might be used to reduce solvation energetics interferences even further, although it is very difficult, if not impossible, to dissolve ionic species in such solvents. Nonetheless, an understanding of the nature of interactions of ionic species with nonpolar aprotic species is of considerable fundamental interest.

The most extensive study of halide interactions with a nonpolar aprotic solvent is that involving interactions with benzene. Hiraoka et al. have undertaken an examination of the clustering reactions between halide ions and benzene via high-pressure mass spectrometry.¹ For the series of halide ions, fluoride was found to bind to benzene with an enthalpy of interaction of 64 kJ/mol, chloride ion by 39 kJ/mol, bromide

ion by 38 kJ/mol, and iodide ion by 26 kJ/mol. Associated low-level computational studies predicted a linear carbon hydrogen halide ion interaction for F^- , Cl^- , and Br^- , while a symmetric simultaneous interaction with two benzene C–H bonds was predicted for I^- . To the best of our knowledge, this remains the only quantitative experimental study of interaction with a hydrocarbon species. However, interestingly, Cody et al. have observed O_2^- clustered with high molecular weight alkanes in an atmospheric pressure chemical ionization experiment.² The only other study exploring interactions of halide ion with hydrocarbons is that of Kebarle which involved a series of aromatic hydrocarbons and dienyl hydrocarbons.³ In these cases the presence of the aromatic ring, or adjacent double bonds, leads to a pronounced enhancement in the acidity of C–H bonds, thus resulting in a strengthened halide–hydrocarbon bond. In the present study an investigation of the energetics of interactions of chloride ions with a series of linear and cyclic alkanes has been undertaken where the C–H bond acidities are all exceedingly low.

■ METHODS

Experimental measurements were made with a pulsed ionization high-pressure mass spectrometer, PHPMS, constructed at the University of Waterloo, which has been described in detail previously.⁴ Due to the weak nature of the bond formed between Cl^- and alkane neutrals, the temperature range was limited to 25–90 °C for the majority of the experiments. Temperatures are accurate to ± 2 °C. Gas mixtures were prepared in a temperature-controlled 5 L reservoir using CH_4 as the bath gas to a pressure of 3–500

Received: April 7, 2013

Revised: June 10, 2013

Published: June 11, 2013



torr and between 50 and 100 torr of the alkane examined. Trace amounts of CCl_4 were added as the chloride source, as shown in eq 1.



The mixture was equilibrated for a minimum of 20 min before being flowed into the ion source at a pressure of 4–6 torr. In the ion source, chloride was produced and reacted with the alkane neutrals to form the $\text{Cl}^-(\text{R}-\text{H})$ complex. Ionization was accomplished by a 50–110 μs pulse of 2 keV electrons focused into the ion source through a 150 μm aperture. Mass-selected ion temporal profiles were monitored by a PC-based multichannel scalar signal acquisition system configured typically at 20 μs dwell time per channel. A total of 250 channels were acquired using a duty cycle 10 ms longer than the residence time for the most persistent ion, which prevents pulse-to-pulse carryover in ion abundance. The results of 500–1000 electron gun pulses were accumulated, dependent on the signal intensity. To ensure that thermal equilibrium was achieved, the pressure dependence of the measured equilibrium constant was determined at several temperatures. Given the relatively high pressure of the alkane clustering reagent, the pressure dependence measurements verify that no additional clustering or dissociation is occurring after the ions exit the ion source. The temperature dependence of the equilibrium constants was obtained by measuring K_{eq} at various ion source temperatures. Van't Hoff plots were then constructed to extract thermochemical data. For example, the Van't-Hoff plot for the chloride–*n*-pentane complex is shown in Figure 1.

Calculations were performed using the Gaussian 09 program package⁵ at the B3LYP⁶ level of theory with a 6-311++G** basis set for initial structural optimization calculations for the neutral alkane (RH) molecules and the $\text{Cl}^-(\text{RH})$ complexes. These initial B3LYP optimized structures were then used for

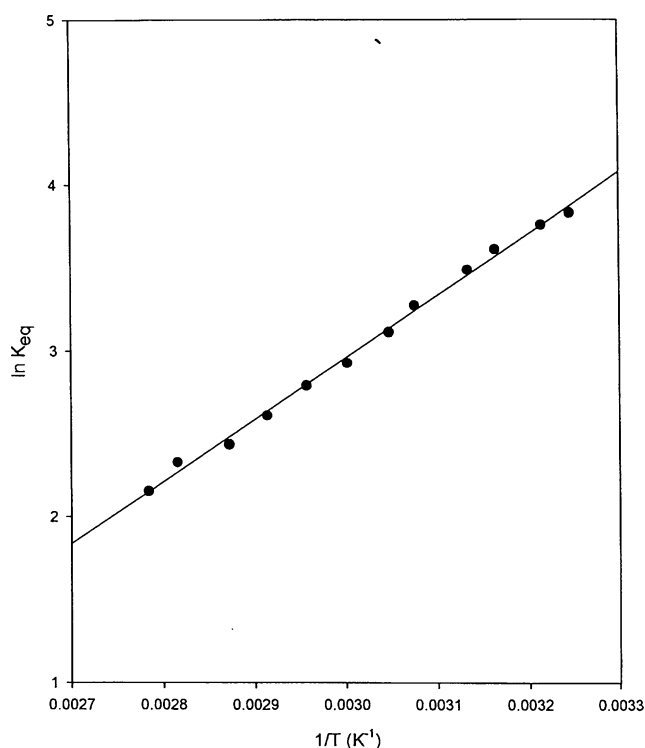


Figure 1. Van't Hoff plot of *n*-pentane–chloride complex.

further geometry optimization and vibrational frequency calculations at the MP2^{7,8}/6-311++G** level of theory. The resulting data, together with the energetics calculated for chloride ion (Cl^-), were then used to calculate the clustering energetics of Cl^- to the relevant alkane. As a test calculation for the accuracy of the computational method, similar calculations were carried out for Cl^- clustering energetics to both methanol and benzene for which accurate previous experimental data are available.^{1,3,4,9–16}

It is well established that anharmonic frequencies, particularly those of the low-frequency modes, will contribute more to the absolute entropy than the default harmonic frequencies. It is important to note, however, that this will apply both to the neutral alkane and the chloride complex. The most significant difference between these will be modes largely associated with interaction with the chloride ion. A calculation has been performed for the chloride–butane case in which the difference in entropy of the chloride–butane complex was found to be 7 J/mol·K with the anharmonic entropy being the higher value, as expected. The difference in entropy for harmonic versus anharmonic absolute entropies for butane is found to be 0.5 J/mol·K. Thus, the difference in ΔS values is only 6.5 J/mol·K which is very small and within the error limits of the experimental measurements. As the alkane molecules become larger, the difference in ΔS values is expected to become less; thus, default harmonic frequencies are considered acceptable for the purposes of this study.

RESULTS AND DISCUSSION

The experimentally obtained association energetics for chloride complexation with the series of *n*-alkanes and cycloalkanes are summarized in Table 1, together with previous experimental and present computational results for chloride complexes of benzene and methanol. The energetics of chloride complexation with each of these latter two molecules were obtained in order to validate the accuracy of the present computational method in reproducing the energetics of interaction. These molecules were chosen since their experimental complexation energetics with chloride are well established.

$\text{CH}_3\text{OH}\cdots\text{Cl}^-$. The most recent experimental results for the interaction of chloride with methanol give enthalpies of binding of 72.8 kJ/mol determined by Hiraoka et al. and 73.2 kJ/mol determined by Bogdanov et al.^{13,17} These are in excellent agreement with the current computed value of 69.9 kJ/mol. Similarly, the corresponding entropy values are 101 and 100 J/mol·K, respectively, also in reasonable agreement with the current computed value of 85 J/mol·K. The computed complexation enthalpy and entropy are also in good agreement with other previous studies.^{3,11,12,15,18,19} The structure of the computed chloride–methanol complex is shown in Figure 2. The O–H and H $\cdots\text{Cl}^-$ distances of 0.99 and 2.08 Å, respectively, and the O–H $\cdots\text{Cl}^-$ bond angle of 167° also agree well with previous computational work by Bogdanov and co-workers.¹⁷

$\text{C}_6\text{H}_6\cdots\text{Cl}^-$. The data for $\text{C}_6\text{H}_6\cdots\text{Cl}^-$ complexes are somewhat more ambiguous. The computational results reveal that there are two complexes relatively close in energy. The first of these, shown in Figure 3a, involves a linear C–H $\cdots\text{Cl}^-$ interaction with a H $\cdots\text{Cl}^-$ hydrogen bond distance of 2.40 Å. The second, somewhat surprising, minimum energy structure, Figure 3b, shows a nonlinear C–H $\cdots\text{Cl}^-$ interaction with a H $\cdots\text{Cl}^-$ hydrogen bond distance of 2.45 Å and a bond angle of 154°. The linear structure is 3.2 kJ/mol enthalpically more

Table 1. Experimental and Theoretical Gas Phase Energetics of Various Chloride Complexes^a

complex	experimental $-\Delta H$ (kJ/mol)	experimental $-\Delta S$ (J/K·mol)	computational $-\Delta H$ (kJ/mol) ^c	computational $-\Delta S$ (J/K·mol)
$\text{Cl}^- + \text{CH}_3\text{OH} \leftrightarrow \text{Cl}^- \cdots (\text{CH}_3\text{OH})$	73.0 ^b	100 ^b	69.9	85
$\text{Cl}^- + \text{C}_6\text{H}_6 \leftrightarrow \text{Cl}^- \cdots (\text{C}_6\text{H}_6)$	39.3 ± 8.4^1	74.9 ¹	37.7	73
$\text{Cl}^- + n\text{-C}_3\text{H}_8 \leftrightarrow \text{Cl}^- \cdots (n\text{-C}_3\text{H}_8)$	N/A	N/A	27.2	83
$\text{Cl}^- + c\text{-C}_3\text{H}_6 \leftrightarrow \text{Cl}^- \cdots (c\text{-C}_3\text{H}_6)$	N/A	N/A	30.2	82
$\text{Cl}^- + n\text{-C}_4\text{H}_{10} \leftrightarrow \text{Cl}^- \cdots (n\text{-C}_4\text{H}_{10})$	N/A	N/A	32.4	82
$\text{Cl}^- + c\text{-C}_4\text{H}_8 \leftrightarrow \text{Cl}^- \cdots (c\text{-C}_4\text{H}_8)$	N/A	N/A	33.1	83
$\text{Cl}^- + n\text{-C}_5\text{H}_{12} \leftrightarrow \text{Cl}^- \cdots (n\text{-C}_5\text{H}_{12})$	37.5	89	37.0	72
$\text{Cl}^- + c\text{-C}_5\text{H}_{10} \leftrightarrow \text{Cl}^- \cdots (c\text{-C}_5\text{H}_{10})$	35.6	83	38.0	95
$\text{Cl}^- + n\text{-C}_6\text{H}_{14} \leftrightarrow \text{Cl}^- \cdots (n\text{-C}_6\text{H}_{14})$	42.6	98	41.5	82
$\text{Cl}^- + c\text{-C}_6\text{H}_{12} \leftrightarrow \text{Cl}^- \cdots (c\text{-C}_6\text{H}_{12})$	40.0	92	41.0	86
$\text{Cl}^- + n\text{-C}_7\text{H}_{16} \leftrightarrow \text{Cl}^- \cdots (n\text{-C}_7\text{H}_{16})$	44.0	97	44.5	84
$\text{Cl}^- + c\text{-C}_7\text{H}_{14} \leftrightarrow \text{Cl}^- \cdots (c\text{-C}_7\text{H}_{14})$	44.0	98	46.0	90
$\text{Cl}^- + n\text{-C}_8\text{H}_{18} \leftrightarrow \text{Cl}^- \cdots (n\text{-C}_8\text{H}_{18})$	49.1	102	46.3	81
$\text{Cl}^- + c\text{-C}_8\text{H}_{16} \leftrightarrow \text{Cl}^- \cdots (c\text{-C}_8\text{H}_{16})$	44.0	102	52.0	95
$\text{Cl}^- + n\text{-C}_9\text{H}_{20} \leftrightarrow \text{Cl}^- \cdots (n\text{-C}_9\text{H}_{20})$	N/A	N/A	50.1	99

^aLevel of theory MP2/6-311++G(d,p). ^bAverage of two values.^{13,17} ^cAll computational values are for the lowest free energy conformers.

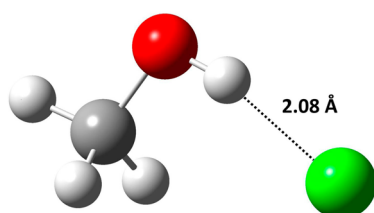


Figure 2. Structure of chloride–methanol complex.

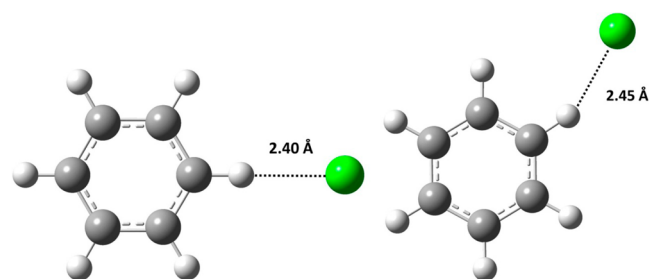


Figure 3. (a, left and b, right) Structures of chloride–benzene complexes.

favorable; however, the nonlinear structure is 5.1 kJ/mol more favorable in terms of Gibbs free energy. Both structures are consistent with the experimental results obtained by Hiraoka.¹ Interestingly, the second structure, more stable in Gibbs free energy, corresponds best with the experimentally obtained energetics of Hiraoka. The experimental enthalpy of association of 39.3 kJ/mol agrees extremely well with the present computational value of 37.7 kJ/mol, while the experimental entropy of association of 74.9 J/mol·K is also in excellent agreement with the present computational value of 73 J/mol·K.^{1,14} These computational data also agree with other experimental data from previous studies.^{15,20,21} This extremely interesting result is consistent with the known tendency of chloride ion to form bent intermolecular hydrogen bonds with other molecules.

The energetics of interaction of chloride ion with cyclopropane, cyclobutane, *n*-propane, and *n*-butane are sufficiently weak that high-pressure mass spectrometry experiments could not be performed since no appreciable intensity of cluster ions

could be observed. However, it is of interest to be able to view the variation of interaction with molecules of increasing carbon number, and therefore, computational studies of these four systems were also performed.

***c*-C₃H₆⋯Cl[−].** The structure of the chloride ion adduct with cyclopropane is shown in Figure 4. As can be seen, the chloride

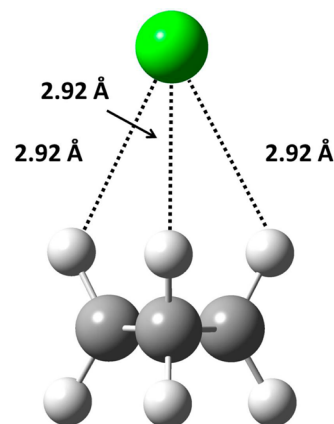


Figure 4. Structure of cyclopropane–chloride complex.

ion sits above the center of the ring with three equal C–H⋯Cl[−] interactions of 2.92 Å. The enthalpy and entropy of interaction are 30.2 kJ/mol and 82 J/mol·K, respectively. The strength of interaction of chloride ion with cyclopropane is such that no change in the C–H bond distances of cyclopropane occurs.

***c*-C₄H₈⋯Cl[−].** The structure of the chloride ion complex with cyclobutane is shown in Figure 5. The cyclobutane ring is slightly folded and the chloride interacts on one face of the ring with two C–H⋯Cl[−] distances of 2.73 Å. The enthalpy and entropy of interaction are 33.1 kJ/mol and 83 J/mol·K, respectively. The chloride interaction does not induce any change in the distortion from nonplanarity of the four-membered ring, and the C–H bond distances similarly remain the same.

***c*-C₅H₁₀⋯Cl[−].** In the lowest energy structure of the chloride–cyclopentane complex, shown in Figure 6a, four of the carbon atoms lie in the same plane. The chloride ion is positioned somewhat symmetrically above the ring such that

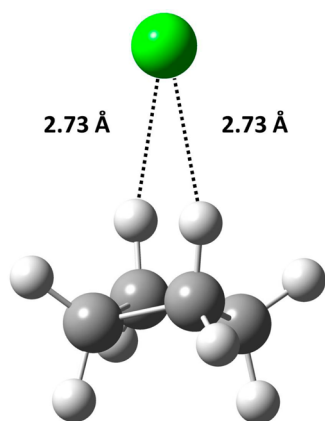


Figure 5. Structure of cyclobutane–chloride complex.

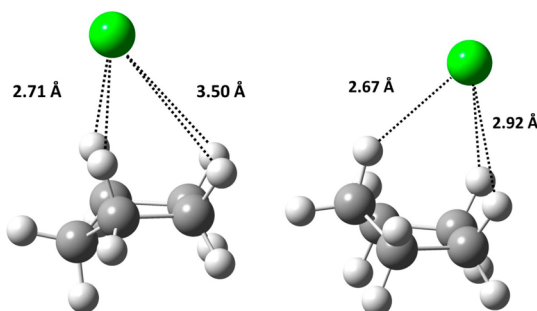


Figure 6. (a, left and b, right) Structures of cyclopentane–chloride complexes.

there are two equidistant C–H...Cl[−] contacts of 2.71 Å and a second pair of equidistant contacts of 3.50 Å. The fifth carbon of the pentane ring lies below the plane of the other four carbons which lie in a common plane. Experimental and theoretical results are in very good agreement with respective enthalpies of binding of 35.6 and 38.0 kJ/mol. Similarly, the respective experimental and computational entropies of association are 83.3 and 95.1 J/mol·K. Computationally, a second structure, shown in Figure 6b, is found which is 2.5 kJ/mol more favorable in enthalpy; however, the entropy of association of 119.4 J/mol·K renders this species 4.7 kJ/mol higher in Gibbs free energy at 298 K which means that at the temperatures of the present experiment the first structure described above is expected to be the more abundant species. This second structure involves the chloride interacting from the other face of the ring with three intermolecular contacts. The out-of-plane C–H interacts with the chloride with a contact distance of 2.67 Å and two additional contacts with hydrogens two carbons removed of 2.92 Å.

c-C₆H₁₂...Cl[−]. The chair conformation of cyclohexane, Figure 7a, gives rise to a simultaneous interaction of chloride ion with the 3 axial hydrogens of one face of the ring with identical C–H...Cl[−] contact distances of 2.73 Å. The experimental and computational energetics are again in excellent agreement with enthalpies of binding of 40 and 41 kJ/mol, respectively, and entropies of binding of 92 and 86 J/mol·K, respectively. It is interesting to compare the analogous structure of chloride ion interacting with the twist-boat conformation of cyclohexane. It is important to note that the “classic” boat structure is actually a transition state between two twist-boat conformers.²² As a result, chloride ion may interact

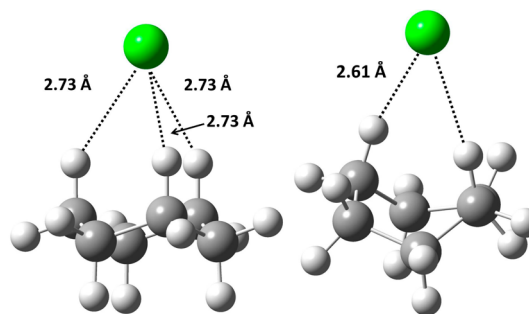


Figure 7. (a, left, and b, right) Structures of cyclohexane–chloride complexes.

equivalently with both faces of the twist-boat. As shown in Figure 7b, this leads to two C–H...Cl[−] contact distances of 2.61 Å in contrast to the four interactions C–H...Cl[−] with contact distances of 2.73 Å in the corresponding complex involving the cyclohexane chair structure. Even though the contacts in the boat conformer complex are shorter, the overall enthalpy of complexation is 26 kJ/mol less favorable than that of the chair conformation complex. Similarly, the entropy of the boat conformer complex is 5 J/mol·K less favorable, resulting in a net difference in ΔG_{298} of ~25 kJ/mol.

c-C₇H₁₄...Cl[−]. The energetically most favorable structure of the chloride complex with cycloheptane is shown in Figure 8.

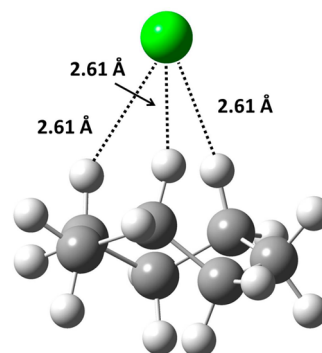


Figure 8. Structure of cycloheptane–chloride complex.

This relatively unsymmetric configuration of the cycloheptane ring gives rise to three unequal C–H...Cl[−] contacts of 2.63, 2.88, and 2.60 Å with the “axial” hydrogens of carbons 1, 3, and 5 of the cycloheptane ring, respectively. All other C–H...Cl[−] distances on the same face of cycloheptane are significantly longer. Excellent agreement is obtained between experimental and computational association energetics with enthalpies of association of 44 and 46 kJ/mol, respectively, and entropies of binding of 98 and 90 J/mol·K, respectively.

c-C₈H₁₆...Cl[−]. The energetically most stable configuration of the chloride cyclooctane complex is shown in Figure 9. This adduct exhibits three identical C–H...Cl[−] contacts of 2.83 Å with the hydrogens of carbons 1, 3, and 6 of the cyclooctane ring interacting with the chloride ion. The next longest C–H...Cl[−] distance is 3.50 Å with a hydrogen of carbon 5. The association energetics are in reasonable agreement with experiment and computational enthalpies of association of 44 and 52 kJ/mol, respectively, and entropies of association of 102 and 95 J/mol·K, respectively.

In comparison to the cycloalkanes, the *n*-alkanes present many more structural possibilities for conformations of both

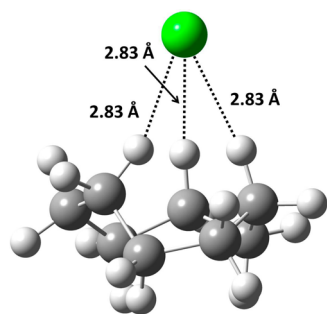


Figure 9. Structure of cyclooctane–chloride complex.

the neutral *n*-alkane and the corresponding chloride complex. Therefore, the energetics of many possible structural motifs have been explored. In the case of the neutral *n*-alkanes, as has been previously determined, the all-trans conformation was found to be the most stable. It has previously been shown in electron diffraction experiments that every change from a trans to a cis conformation for the short-chain alkanes examined in the present work results in an increase of ~ 2.5 kJ/mol in Gibbs free energy.²³ However, for purposes of this study, computational energetics are given with respect to the all-trans conformation of the *n*-alkane. For the chloride–alkane complexes, the most energetically favorable motifs are described. Undoubtedly, minor variations due to small chain distortions may exist.

***n*-C₃H₈...Cl[−].** The structure of chloride ion complexed with *n*-propane is shown in Figure 10. In this structure, the chloride

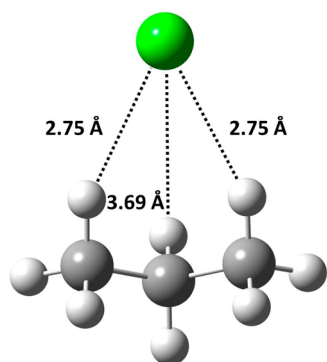


Figure 10. Structure of *n*-propane–chloride complex.

ion sits between carbons 1 and 2 and has two equal C–H...Cl[−] contacts of 2.75 Å with the hydrogens of these carbons. A third C–H...Cl[−] contact involving carbon 3 has a length of 3.69 Å. The computationally determined enthalpy and entropy of complexation are 27.2 kJ/mol and 83 J/mol·K, respectively.

***n*-C₄H₁₀...Cl[−].** The complex of *n*-butane and chloride ion is shown in Figure 11. The chloride ion sits above the alkane chain with C–H...Cl[−] contacts to carbons 1–4 of 2.86, 3.32, 2.68, and 3.87 Å, respectively. The computationally determined enthalpy and entropy of interaction are 32.4 kJ/mol and 82 J/mol·K, respectively. The structure shown in Figure 11 represents an anti configuration of the terminal methyl groups. A gauche structure was also examined and was found to be 4.5 kJ/mol higher in free energy relative to the anti structure, which means that it would represent roughly 15% in a statistical population of structures. For the purposes of this work, only the most stable anti structures have been reported.

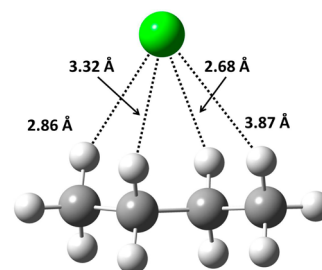


Figure 11. Structure of *n*-butane–chloride complex.

***n*-C₅H₁₂...Cl[−].** An exploration of the potential energy surface for chloride complexes of *n*-pentane leads to two structural possibilities, which are more energetically favorable than all others. These two structures are shown in Figure 12a and 12b, which differ in enthalpy by only ~ 1 kJ/mol. However, significantly, the entropies of these two complexes differ by 18 J/mol·K, which is sufficient that under the present experimental conditions structure 12a would be predominant. In terms of sites of interaction of the chloride ion with the hydrogens of the chain, distances of 3.13, 3.21, 2.65, 3.36, and 3.79 Å for the hydrogens of carbons 1–5, in that order, are found for structure 12a. Correspondingly, distances of 2.91 and 4.14 Å are found for interaction at the hydrogens of carbon 1, 2.65 Å at carbon 3, 3.34 Å at carbon 4, and 3.00 Å at carbon 5. As a result of these two patterns of interactions, structure 12b exhibits overall greater interactions at the two methyl termini than is the case for structure 12a, giving rise to greater restriction of internal rotations of the methyl termini. Thus the two structures, while very close in enthalpy, become sufficiently different in Gibbs free energy that structure 12a predominates with less than 5% of 12b present at the lowest temperature of the experiment and diminishing amounts of 12b present as the temperature increases. The experimental and computational results are in good agreement with the two methods yielding enthalpies of association of 37.5 and 37.0 kJ/mol, respectively. The entropies similarly agree quite well with experimental and computational values of 89 and 72 J/mol·K, respectively.

***n*-C₆H₁₄...Cl[−].** The experimentally determined values for the interaction of chloride ion with *n*-hexane give an enthalpy and entropy of interaction of 42.6 kJ/mol and 98 J/mol·K, respectively. Computationally, four relatively low-energy structures, which differ in energy by only ~ 8 kJ/mol, were located for the chloride ion complex with *n*-hexane. These are shown in Figures 13a–d. The structure, 13a, which is lowest in enthalpy, is also the most favorable in terms of entropy and involves a hexane chain that remains essentially linear. The extent to which it is nonlinear can be defined by the dihedral angle created by the central four carbons atoms of the chain which, in this case, is 171°. This structure involves three relatively close contacts to hydrogens of the hexane chain with a contact of 2.87 Å at carbon 2 and 3.07 Å at carbon 3 and 2.70 Å at carbon 4. The distances to the hydrogens at carbons 1, 5, and 6 are 4.03, 3.54, and 4.12 Å, respectively, none of which would seem to be sufficiently strong to inhibit internal rotations. The computational enthalpy and entropy of interaction found for this conformation are 41.5 kJ/mol and 82 J/mol·K. The next lowest energy structure, 13b, involves C–H...Cl[−] contacts of 3.88, 2.83, 3.09, and 2.76 Å at carbons 1–4 respectively. No close contact is exhibited for hydrogens at carbon 5; however, at carbon 6 an additional contact of 3.05 Å is seen which indicates that the chain is beginning to fold

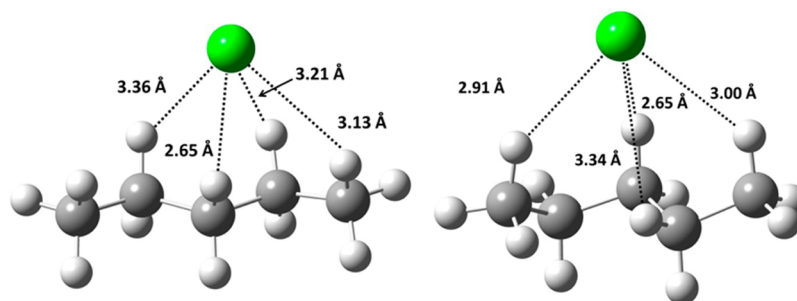


Figure 12. (a, left, and b, right) Structures of *n*-pentane–chloride complexes.

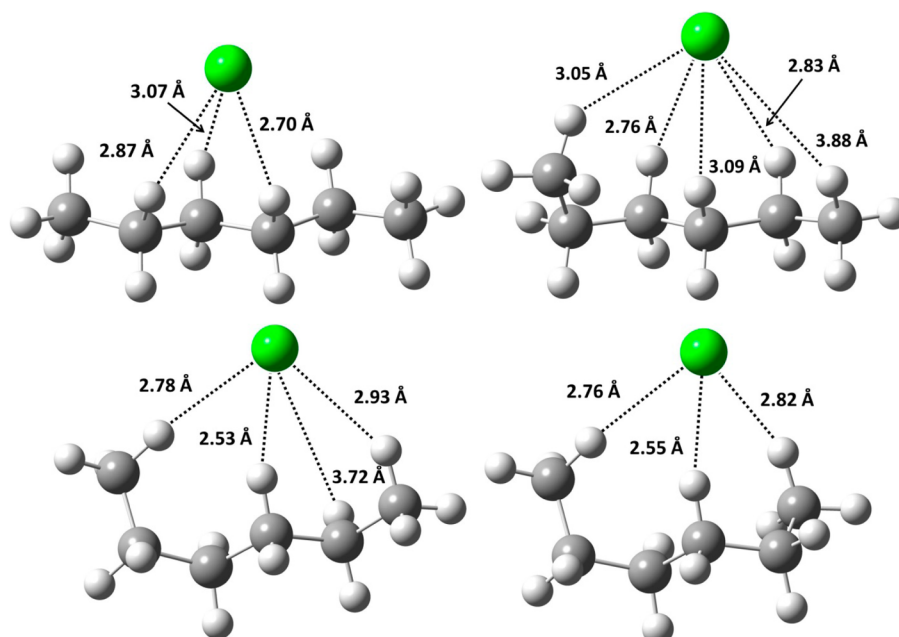


Figure 13. (a, top left, b, top right, c, bottom left, and d, bottom right) Structures of *n*-hexane–chloride complexes.

around the chloride ion. The computational enthalpy and entropy of association for structure 13b are 40.8 kJ/mol and 90 J/mol·K, respectively. The structure, 13c, found to be next lowest in energy exhibits a folding of the chain at both ends to appear to wrap around the chloride ion. The contacts at carbon 1–4 are 2.93, 3.72, 2.53, and 4.29 Å, respectively; no contact at carbon 5 is made, and a contact of 2.78 at carbon 6 is observed. The computational enthalpy and entropy of association for structure 13b are 40.0 kJ/mol and 92 J/mol·K, respectively. The fourth and final structure, 13d, considered in the present work exhibits a continued distortion of the C6 chain from linearity and involves C–H···Cl[−] contacts of 2.82 Å at carbon 1, 2.55 Å at carbon 3, and 2.76 Å at carbon 6. Notably, no close contacts exist at carbons 2, 4, and 5. The computational enthalpy and entropy of association for structure 13d are 37.4 kJ/mol and 96 J/mol·K, respectively. Assuming that the above energetics are correct, the populations of the four structures would be roughly 67, 22, and 11% for structures 13a–c, respectively. No appreciable amount of structure 13d would be expected. The experimental measurements would be sampling such a mixture, and the weighted average of the computed structures of the computed structures is thus seen to be in good agreement with the experimental values.

***n*-C₇H₁₆···Cl[−].** The experimentally determined values for the interaction of chloride ion with *n*-hexane give an enthalpy and entropy of interaction of 44.0 kJ/mol and 97 J/mol·K,

respectively. The three computationally determined lowest energy structures representing the main possible structural motifs are shown in Figures 14a–c. The lowest energy structure found, 14a, resembles that found for *n*-hexane in that it retains a relatively linear chain structure. In this case, the curvature of the chain as defined by the dihedral angle of either of the

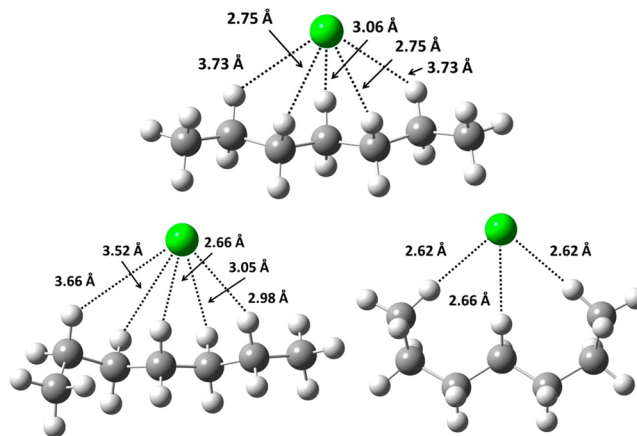


Figure 14. (a, top, b, bottom left, and c, bottom right) Structures of *n*-heptane–chloride complexes.

central four atoms is the same as that observed in *n*-hexane at 171° . In this structure, the $\text{C-H}\cdots\text{Cl}^-$ contacts of importance are 3.73, 2.75, 3.06, 2.75, and 3.73 Å at carbons 2–6, respectively, giving rise to a symmetric interaction with respect to the carbon chain. Computationally, the enthalpy and entropy of interaction for this structure is found to be 44.5 kJ/mol and 84 J/mol·K, respectively. Structure **14b** involves a curvature of the carbon chain which is relatively unchanged with the difference now that the methyl group at carbon 1 is rotated away from the chloride ion by what is essentially a rotation about the carbon 2–carbon 3 axis. The $\text{C-H}\cdots\text{Cl}^-$ contacts of importance are 2.98, 3.05, 2.66, 3.52, and 3.66 Å for carbons 2–6 respectively. Computationally, the enthalpy and entropy of complexation for this structure are found to be 41.7 kJ/mol and 82 J/mol·K, respectively. The final structural motif of interest, structure **14c**, involves a significant folding of the carbon chain around the chloride such that a symmetric structure results with $\text{C-H}\cdots\text{Cl}^-$ interactions of 2.62 Å with each of the terminal methyl groups and a central $\text{C-H}\cdots\text{Cl}^-$ interaction of 2.66 Å at carbon 4. No significant interactions occur at carbons 2, 3, 5, and 6. This structure gives rise to an enthalpy and entropy of interaction of 43.7 kJ/mol and 103 J/mol·K, respectively. It is of interest to note the significant loss in entropy of structure **14c**, as a result of the restriction of internal rotations of the terminal methyl groups. In this case, the computational energetics appear to be slightly more favorable than the values determined by experiment.

***n*-C₈H₁₈⋯Cl[−].** Experimentally the enthalpy and entropy of interaction of chloride ion with *n*-octane are found to be 49.1 kJ/mol and 102 J/mol·K, respectively. Computationally, the three lowest energy structures found for chloride interaction with *n*-octane are shown in Figures 15a–c. The most energetically favorable structure found, **15a**, retains the linear-type structure found for previous normal alkanes investigated in the present work. This structure has no significant $\text{C-H}\cdots\text{Cl}^-$ contacts at the terminal methyl groups nor at the methylene group of carbon 7, but the $\text{C-H}\cdots\text{Cl}^-$ interaction from carbon 2–6 are 3.82, 2.79, 3.04, 2.73, 3.53 Å, respectively. The curvature of the carbon chain as defined by the dihedral angle created by either pair of the central 4 carbon atoms is 168° . This structure gives rise to an enthalpy and entropy of interaction of 46.3 kJ/mol and 81 J/mol·K, respectively. The second of the three structures, structure **15b**, is shown in Figure 15b and has a computational enthalpy and entropy of complexation of 44.7 kJ/mol and 82 J/mol·K, respectively. This structure exhibits an S-shape with the chloride ion residing at the center of the S between carbons 3 and 4. The $\text{C-H}\cdots\text{Cl}^-$ contacts in this structure occur at carbon 1, 3, 4, 5, 6, and 7 with lengths of 3.35, 3.17, 2.82, 2.78, 3.33, and 3.70 Å. No significant contacts occur at carbon 2, nor 8. A further structure, **15c**, which is analogous to structure **13c** of the *n*-hexane–chloride complex, is shown in Figure 15c with a computational enthalpy and entropy of interaction of 46.3 kJ/mol and 97 J/mol·K, respectively. The $\text{C-H}\cdots\text{Cl}^-$ contacts in this structure occur at carbon 1, 4, 5, 6, and 8 with lengths of 2.87, 2.63, 3.22, 2.81, and 3.19 Å. No significant contacts occur at carbon 2, 3, nor 7. The agreement between experimental and computational energetics for *n*-octane is very good.

***n*-C₉H₂₀⋯Cl[−].** The lowest energy structure of the *n*-nonane–chloride ion complex is shown in Figure 16. It was calculated to confirm a trend emerging from the smaller *n*-alkanes in which a diminishing increase is observed in binding energy compared to the *c*-alkanes. The structure of the *n*-

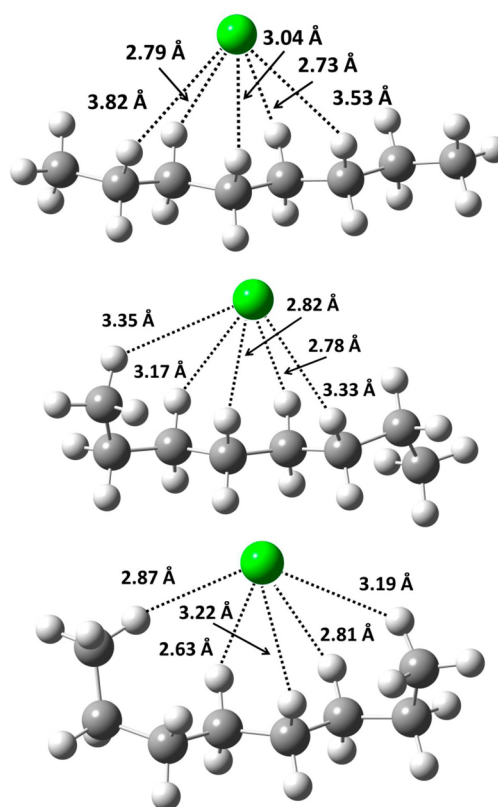


Figure 15. (a, top, b, middle, and c, bottom) Structures of *n*-octane–chloride complexes.

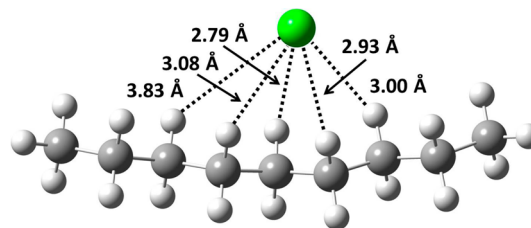


Figure 16. Structure of *n*-nonane–chloride complex.

nonane complex also follows the trend of other normal alkanes in the series with the alkane exhibiting a mostly linear structure and chloride interacting at the center of the linear alkane. The $\text{C-H}\cdots\text{Cl}^-$ contacts in this structure occur at carbon 3, 4, 5, 6, and 7 with lengths of 3.00, 2.93, 2.79, 3.08, and 3.83 Å. No significant contacts occur at carbon 1, 2, 8, nor 9. The computational enthalpy and entropy of complexation are 50.1 kJ/mol and 99 J/mol·K, respectively.

It is of considerable interest to examine the correlation between the enthalpy of binding and the size of the alkane. In Figure 17, a plot of computationally determined ΔH of interaction of chloride ion with each of the alkanes as a function of carbon number is displayed. It is clear that there is an excellent correlation between alkane size and the strength of the interaction with chloride ion. The alkanes are nonpolar molecules, and the interaction with the chloride ion, which can be considered to approximate a point charge, is dominated by the charge-induced dipole interaction. The strength of the ion-induced dipole interaction with chloride is, therefore, a direct function of the polarizability of the alkane. A plot of the computationally determined enthalpy of interaction as a

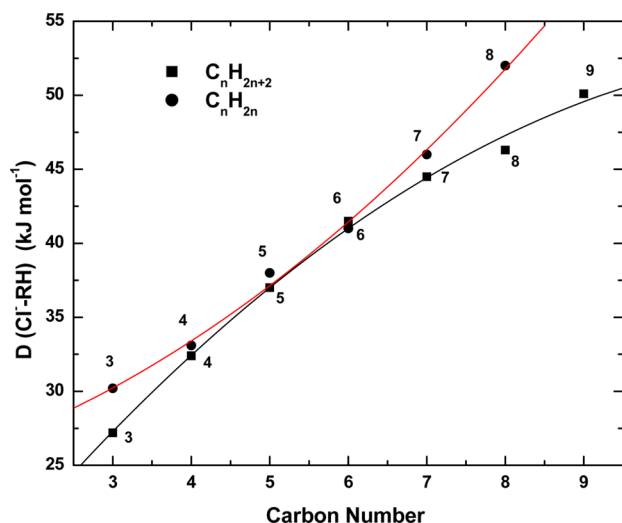


Figure 17. Plot of the computationally determined enthalpy of interaction compared to the number of carbons of normal and cycloalkanes complexed to chloride ion at 298 K. Level of theory MP2/6-311++G(d,p). Fit lines are polynomial in nature and merely intended to guide the eye and do not represent any physical information.

function of polarizability is presented in Figure 18. This plot shows very good correlation for the cycloalkanes; however, for

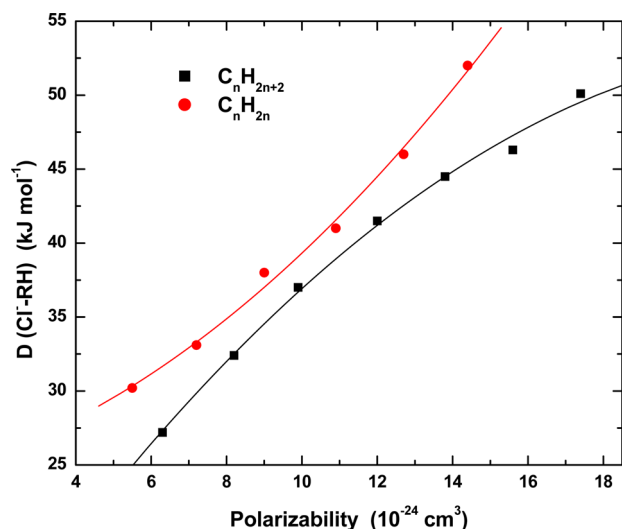


Figure 18. Plot of computationally determined enthalpy of interaction compared to the polarizability of normal and cycloalkanes complexed to chloride ion at 298 K. Level of theory MP2/6-311++G(d,p).²⁴ Fit lines are polynomial in nature and merely intended to guide the eye and do not represent any physical information.

the *n*-alkanes, a diminished increase in enthalpy of interaction begins to be apparent at the higher carbon numbers. This can be considered to be the direct result of the fact that the chloride ion cannot simultaneously interact with the same strength at all parts of the alkane chain. As the *n*-alkane chain length increases, the deviation is expected to become increasingly pronounced.

CONCLUSION

The experimental and computational determinations of the energetics of interaction of chloride ion with nonpolar alkane molecules carried out in the present work demonstrate that the

level of theory used for the computations provides a very accurate reproduction of the experimental values. The structural insight gained provides considerable understanding of the effect of a negative charge center on the conformation of a normal or cycloalkane. The enthalpy of interaction between chloride and the alkane neutrals increases with increasing carbon number and increasing polarizability which demonstrates that the interaction is largely electrostatic as the result of an ion-induced dipole potential. This investigation also illustrates the sensitivity and accuracy of the high-pressure mass spectrometric equilibrium method to probe weak ion–molecule interactions in the gas phase.

AUTHOR INFORMATION

Corresponding Author

*E-mail: mcmahon@uwaterloo.ca.

Notes

The authors declare no competing financial interest.

ACKNOWLEDGMENTS

The generous financial support of the Natural Sciences and Engineering Research Council is gratefully acknowledged. This work was made possible by the facilities of the Shared Hierarchical Academic Research Computing Network (SHARCNET:www.sharcnet.ca) and Compute/Calcul Canada.

REFERENCES

- (1) Hiraoka, K.; Mizuse, S.; Yamabe, S. Determination of the Stabilities and Structures of X-(C₆H₆) Clusters (X = Cl, Br, and I). *Chem. Phys. Lett.* **1988**, *147*, 174–178.
- (2) Cody, R. B.; Dane, A. J. Soft Ionization of Saturated Hydrocarbons, Alcohols, and Nonpolar Compounds by Negative-Ion Direct Analysis in Real-Time Mass Spectrometry. *J. Am. Soc. Mass Spectrom.* **2013**, *24*, 329–34.
- (3) French, M. A.; Ikuta, S.; Kebarle, P. Hydrogen Bonding of O–H and C–H Hydrogen Donors to Cl[−]. Results from Mass Spectrometric Measurements of the Ion–Molecule Equilibria RH + Cl[−] = RHCl[−]. *Can. J. Chem.* **1982**, *60*, 1907–1918.
- (4) Szulejko, J. E.; Fisher, J. J.; McMahon, T. B.; Wronka, J. A Pulsed Ionization High-Pressure Mass-Spectrometric Study of Methyl Cation Transfer and Methyl Cation-Induced Clustering in Dimethyl Ether–Acetone Mixtures. *Int. J. Mass Spectrom. Ion Processes* **1988**, *83*, 147–161.
- (5) Frisch, M. J.; Trucks, G. W.; Schlegel, H. B.; Scuseria, G. E.; Robb, M. A.; Cheeseman, J. R.; Scalmani, G.; Barone, V.; Mennucci, B.; Petersson, G. A.; et al. *Gaussian 09*, revision A.1; Gaussian, Inc.: Wallingford, CT, 2009.
- (6) Becke, A. D. Density-Functional Thermochemistry. III. The Role of Exact Exchange. *J. Chem. Phys.* **1993**, *98*, 5648–5652.
- (7) Moller, C.; Plesset, M. S. Note on an Approximation Treatment for Many-Electron Systems. *Phys. Rev.* **1934**, *46*, 618–622.
- (8) Head-Gordon, M.; Pople, J. A.; Frisch, M. J. MP2 Energy Evaluation by Direct Methods. *Chem. Phys. Lett.* **1988**, *153*, 503–506.
- (9) Yamdagni, R.; Kebarle, P. Solvation of Negative Ions by Protic and Aprotic Solvents. Gas-Phase Solvation of Halide Ions by Acetonitrile and Water Molecules. *J. Am. Chem. Soc.* **1972**, *94*, 2940–43.
- (10) Yamdagni, R.; Kebarle, P. Hydrogen-Bonding Energies to Negative Ions from Gas-Phase Measurements of Ionic Equilibria. *J. Am. Chem. Soc.* **1971**, *93*, 7139–7143.
- (11) Yamdagni, R.; Payzant, J. D.; Kebarle, P. Solvation of Cl[−] and O^{2−} with H₂O, CH₃OH, and CH₃CN in the Gas Phase. *Can. J. Chem.* **1973**, *51*, 2507–2511.
- (12) Evans, D. H.; Keesee, R. G.; Castleman, A. W., Jr. Thermodynamics of Gas-Phase Mixed-Solvent Cluster Ions: Water

and Methanol on K^+ and Ci^- and Comparison to Liquid Solutions. *J. Phys. Chem.* **1991**, 95, 3558–3564.

(13) Hiraoka, K.; Mizuse, S. Gas Phase Solvation of Cl^- with H_2O , CH_3OH , C_2H_5OH , $i-C_3H_7OH$, $n-C_3H_7OH$, and $t-C_4H_9OH$. *Chem. Phys.* **1987**, 118, 457–466.

(14) Larson, J. W.; McMahon, T. B. Gas Phase Negative Ion Chemistry of Alkylchloroformates. A Convenient Method for Bimolecular Generation of Chloride Ion Adducts and Determination of Chloride Affinities from Ion Cyclotron Resonance Thermal Equilibrium Measurements. *Can. J. Chem.* **1984**, 62, 675–679.

(15) Larson, J. W.; McMahon, T. B. Hydrogen Bonding in Gas-Phase Anions. An Experimental Investigation of the Interaction between Chloride Ion and Bronsted Acids from Ion Cyclotron Resonance Chloride Exchange Equilibria. *J. Am. Chem. Soc.* **1984**, 106, 517–521.

(16) Riveros, J. M.; Breda, A. C.; Blair, L. K. Formation and Relative Stability of Chloride Ion Clusters in the Gas Phase by Ion Cyclotron Resonance Spectroscopy. *J. Am. Chem. Soc.* **1973**, 95, 4066–67.

(17) Bogdanov, B.; Peschke, M.; Tonner, D. S.; Szulejko, J. E.; McMahon, T. B. Stepwise Solvation of Halides by Alcohol Molecules in the Gas Phase. *Int. J. Mass Spectrom.* **1999**, 185/186/187, 707–725.

(18) Yamabe, S.; Furumiya, Y.; Hiraoka, K.; Morise, K. Theoretical Van't Hoff Plots of Gas-Phase Ion Equilibria of Chloride Ion in Water, Methanol, and Acetonitrile. *Chem. Phys. Lett.* **1986**, 131, 261–66.

(19) Sieck, L. W. Thermochemistry of Solvation of NO_2^- and $C_6H_5NO_2$ by Polar Molecules in the Vapor Phase. Comparison with Cl^- and Variation with Ligand Structure. *J. Phys. Chem.* **1985**, 89, 5552–5556.

(20) Paul, G. J. C.; Kebarle, P. Stabilities of Complexes of Br^- with Substituted Benzenes (SB) Based on Determinations of the Gas-Phase Equilibria $Br^- + SB = (BrSB)$. *J. Am. Chem. Soc.* **1991**, 113, 1148–1154.

(21) Sunner, J.; Nishizawa, K.; Kebarle, P. Ion–Solvent Molecule Interactions in the Gas-Phase—The Potassium–Ion and Benzene. *J. Phys. Chem.* **1981**, 85, 1814–1820.

(22) Nelson, D. J.; Brammer, C. N. Toward Consistent Terminology for Cyclohexane Conformers in Introductory Organic Chemistry. *J. Chem. Educ.* **2010**, 88, 292–294.

(23) Bartell, L. S.; Kohl, D. A. Structure and Rotational Isomerization of Free Hydrocarbon Chains. *J. Chem. Phys.* **1963**, 39, 3097–3105.

(24) Miller, K. J. Calculation of the Molecular Polarizability Tensor. *J. Am. Chem. Soc.* **1990**, 112, 8543–8551.